BMP7 expression in the adult rat brain

Yuya Kusakawa [a,b], Sumiko Mikawa [a], Kohji Sato [a,*]

[a] *Department of Tissue & Organ Anatomy, Hamamatsu University School of Medicine, 1-20-1 Handayama, Higashiku, Hamamatsu, Shizuoka 431-3192, Japan*
[b] *AICHI Medical College for Physical and Occupational Therapy, 519 Ichiba, Kiyosu, Aichi 452-0931, Japan*

ARTICLE INFO

ABSTRACT

Bone morphogenetic protein-7 (BMP7), a member of the transforming growth factor-β (TGF-β) super-family, has various effects in many biological events. However, there is little information on BMP7 expression in the adult central nervous system (CNS). Therefore, we investigated BMP7 levels in the adult rat CNS using immunohistochemistry. Abundant BMP7 expression was seen in astrocytes through-out the CNS and strong BMP7 expression was also observed in neuropils of the gray matter. Furthermore, BMP7 expression was observed in several kinds of neurons, including oxytocin, dopaminergic and nora-drenergic neurons. These data suggest that BMP7 is widely expressed throughout the adult CNS, and support the idea that BMP7 plays pivotal roles in the adult brain, as well as in the developing brain.

1. Introduction

Bone morphogenetic proteins (BMPs) are multifunctional cytokines involved in the development and differentiation of var-ious tissues, including mesoderm induction and nerve formation and apoptosis (Bragdon et al., 2011). To date, about 20 BMPs have been identified and they form the largest group in the TGF-β fam-ily. BMP receptors are present in the cell membrane as two types of serine/threonine kinase receptors (types I and II) that are essen-tial for transmission of BMP signals (Bragdon et al., 2011). Different combinations of type I and type II receptors have different affini-ties for BMP ligands (Bragdon et al., 2011). Activation of type I receptors by type II receptors leads to phosphorylation of receptor-activated Smads (R-Smads; Smad1/5/8), and the phosphorylated R-Smads bind to the common-mediator Smad (Co-Smad; Smad4) (Moustakas and Heldin, 2009). The Smad complexes are trans-ported into the nucleus and regulate the expression of BMP target genes. BMPs also activate Smad-independent signaling pathways, such as the MAP kinase pathway (Massague, 2003), and BMP signals are inhibited by secreted proteins that bind to BMPs, such as noggin, chordin, and neurogenesin-1 (Cho and Blitz, 1998; Ueki et al., 2003).

BMP7, a member of the TGF-β superfamily, is widely expressed in thymus, bone marrow, spleen, brain, spinal cord, heart, skeletal muscle, kidney, lung, liver, pancreas, and prostate (Bragdon et al., 2011). BMP7 homozygous mutants exhibit many specific skeletal defects with variable penetrance, including abnormalities associ-ated with development of the renal and ocular systems (Dudley et al., 1995). In the central nervous system (CNS), BMP7 regulates astrocytes. For example, Yanagisawa et al. (2001) have shown that BMP7 inhibits neurogenesis and induces astrocytogenesis of mouse fetal neuroepithelial cells. In the developing cerebral cortex, BMP7 induces radial glia differentiation and blocks neuronal migration (Ortega and Alcantara, 2010). Furthermore, Jordan et al. (1997) showed that application of BMP7 to rat mesencephalic cell cultures increased both the number of tyrosine hydroxylase-expressing cells and dopamine uptake. Moreover, BMP7 has been shown to promote dendritic growth in sympathetic neurons (Courter et al., 2016). These reports suggest that BMP7 plays pivotal roles in the CNS, but there is little information on the distribution of BMP7 in the adult CNS. Therefore, this distribution was investigated in this study.

2. Experimental procedures

2.1. Animals and section preparation

Wistar male rats (n = 8, 7 weeks old; Japan SLC Inc., Shizuoka, Japan) of 7 weeks of age were used in the study. Under deep

anesthesia, rats were perfused and fixed with 0.1 M phosphate buffer (PB, pH 7.4) containing 4% paraformaldehyde and 0.2% picric acid, and then the brains were quickly excised, postfixed with the same fixative solution for 2 h at 4 °C, and immersed in 10%, 20%, and 25% sucrose overnight at 4 °C, respectively. Samples were frozen and cut using a cryostat. Sections for immunoperoxidase staining were 20 μm thick and those for immunofluorescence staining were 10 μm. Serial sections of 5 μm were used for the mirror method. This study was performed according to the Guidelines for Animal Experimentation at Hamamatsu University School of Medicine.

2.2. Immunohistochemistry (IHC)

For immunoperoxidase staining, slices were blocked with 10% normal goat serum, 2% bovine serum albumin (BSA) and 0.2% Triton X-100 in 0.1 M PB for 2 h at room temperature (RT), and then incubated with rabbit anti-BMP7 antibody (diluted 1:500, final concentration, 2 μg/ml; Sigma-Aldrich, St. Louis, MO) or rabbit anti-oxytocin antibody (diluted 1:30000, initial concentration not available; Immunostar, Hudson, WI) overnight at 4 °C. After rinsing with 0.1 M PB, the slices were incubated in goat anti-rabbit IgG with peroxidase complex (no dilution, ready-to-use; EnVision™ System, K4002; DAKO, Tokyo, Japan) for 2 h at RT. After rinsing with 0.1 M PB, 3, 3′-diaminobenzidine (Wako, Osaka, Japan) was used as a substrate for visualization. IHC for controls was performed similarly, but without anti-BMP7 antibody.

For immunofluorescence staining with rabbit anti-BMP7 antibody (diluted 1:500; final concentration, 2 μg/ml; Sigma-Aldrich), slices were blocked with 10% normal goat serum, 2% BSA and 0.2% Triton X-100 in 0.1 M PB for 2 h at RT, and incubated with rabbit anti-BMP7 antibody overnight at 4 °C. After rinsing with 0.1 M PB, slices were incubated with Alexa Fluor 594 goat anti-rabbit IgG (diluted 1:500; final concentration, 4 μg/ml; Molecular Probes, Eugene, OR) for 1.5 h at RT. For double immunofluorescence staining with rabbit anti-BMP7 antibody and mouse anti-glial fibrillary acidic protein (GFAP) antibody (Millipore, Temecula, CA), slices were blocked with 10% normal goat serum, 2% BSA and 0.2% Triton X-100 in 0.1 M PB for 2 h at RT, and then incubated with rabbit anti-BMP7 antibody (diluted 1:500; final concentration, 2 μg/ml) and mouse anti-GFAP antibody (diluted 1:1000; initial concentration not available) overnight at 4 °C. After rinsing with 0.1 M PB, slices were incubated with both Alexa Fluor 594 goat anti-rabbit IgG (diluted 1:500; final concentration, 4 μg/ml) and Alexa Fluor 488 goat anti-mouse IgG (diluted 1:500; final concentration, 4 μg/ml; Molecular Probes) for 1.5 h at RT. For double immunofluorescence staining with rabbit anti-BMP7 antibody and goat anti-Iba1 antibody (Abcam plc, Cambridge, UK), slices were blocked with 10% normal donkey serum, 2% BSA and 0.2% Triton X-100 in 0.1 M PB for 2 h at RT, and incubated with rabbit anti-BMP7 antibody (diluted 1:500; final concentration, 2 μg/ml) and goat anti-Iba1 antibody (diluted 1:1000; final concentration, 1 μg/ml) overnight at 4 °C. After rinsing with 0.1 M PB, slices were incubated with both Alexa Fluor 594 donkey anti-rabbit IgG (diluted 1:500; final concentration, 4 μg/ml; Molecular Probes) and Alexa Fluor 488 donkey anti-goat IgG (diluted 1:500; final concentration, 4 μg/ml; Molecular Probes) for 1.5 h at RT. At the end of the protocol, samples were mounted in ProLong Diamond Antifade Mountant with DAPI (Molecular Probes).

Bright field images were obtained using a microscope (Eclipse 80i; Nikon, Tokyo, Japan) equipped with a CCD camera (DS-Ri; Nikon). Fluorescence images were obtained using a microscope (Eclipse E-600; Nikon) equipped with the same CCD camera and further processed using Adobe Photoshop (Tokyo, Japan).

2.3. Western blotting

A whole rat brain was homogenized in 50 mM Tris-HCl (pH 7.4) buffer containing protease inhibitor cocktail (Nacalai Tesque, Kyoto, Japan) to avoid protein denaturation, and added to 2 × SDS-PAGE sample buffer for solubilization. The sample was used for SDS-PAGE (14% acrylamide; PAGEL, ATTO Corp., Tokyo, Japan). SDS-PAGE products were transferred to a PVDF membrane (Immobilon-P; Merck Millipore, Tokyo, Japan) by electroblotting (40 V overnight at 4 °C) using a transfer buffer (25 mM Tris, 192 mM glycine) containing 20% methanol. The membranes were treated with 3% BSA in 50 mM Tris-buffered saline containing 0.05% Tween-20 (TTBS) for 2 h at RT and then incubated with rabbit anti-BMP7 antibody (diluted 1:600; final concentration, 1.67 μg/ml; Sigma-Aldrich) in TTBS containing 1% BSA for 40 min at RT. After rinsing with TTBS, the blots were incubated with horseradish peroxidase-linked goat anti-rabbit IgG (diluted 1:2000; final concentration, 1 μg/ml; Nacalai Tesque) in TTBS containing 1% BSA for 40 min at RT. After rinsing the blots with TTBS several times, signals were visualized using a SuperSignal West Pico chemiluminescent Substrate (Thermo Fisher Scientific, Waltham, MA).

3. Results

Western blotting was performed to investigate whether the rabbit anti-BMP7 antibody specifically recognizes BMP7. As shown in Fig. 1A, western blotting with the antibody against whole rat brain gave a single band of about 48 kDa, which is consistent with the calculated size. IHC performed without the first antibody (Fig. 1B and C) showed no staining. These data clearly indicate that the rabbit anti-BMP7 antibody recognizes BMP7 protein.

3.1. General expression patterns

An overview of BMP7 expression in adult rat brain is shown in Fig. 2. BMP7-like immunoreactivity (IR) was seen throughout the brain, including abundant BMP7-IR in the olfactory bulb (Fig. 2A), basal ganglia (Fig. 2B), cerebral cortex (Fig. 2B–E), hippocampus (Fig. 2C–E), thalamus (Fig. 2C and D), hypothalamus (Fig. 2D and E), midbrain (Fig. 2E), cerebellum (Fig. 2F and G), brainstem (Fig. 2F–H), and spinal cord (Fig. 2I). A summary of the relative intensities of BMP7-IR in the rat CNS is given in Table 1.
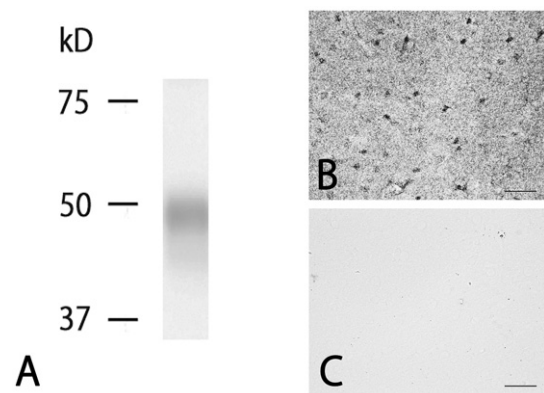

Fig. 1. Specificity of the anti-BMP7 antibody. Western blot analysis using anti-BMP7 antibody for whole rat brain gave a single band of about 48 kDa (A). Immunostaining with anti-BMP7 antibody (B) without the first antibody (C) in the cerebral cortex. Immunostaining without the first antibody gave no significant signals. Scale bar = 40 μm for B, C.
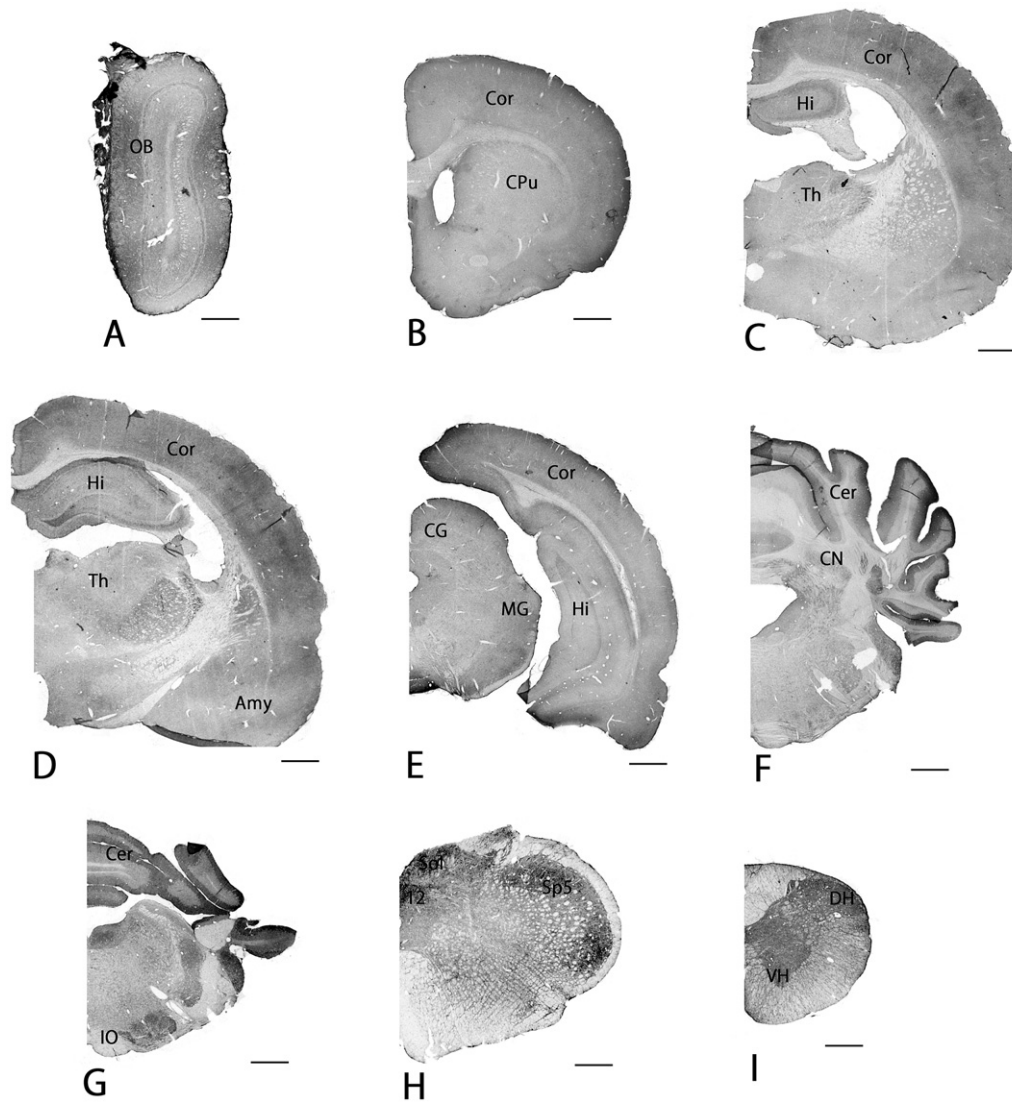
Fig. 2. BMP7 expression in whole rat brain (A–I). 12, hypoglossal nucleus; Amy, amygdala; Cer, cerebellar cortex; CG, central gray; CN, cerebellar nuclei; Cor, cerebral cortex; CPu, caudate putamen; DH, dorsal horn; Hi, hippocampus; IO, inferior olive; MG, medial geniculate; OB, olfactory bulb; Sol, nucleus of the solitary tract; Sp5, spinal trigeminal nucleus; Th, thalamus, VH, ventral horn. Scale bar = 0.5 mm for A, H, I; 1 mm for B-G.

3.2. Telencephalon

3.2.1. Olfactory bulb

Strong BMP7 expression was found in the olfactory nerve layer, with moderate expression in other layers (Fig. 3A). Closer observation showed strongly stained astrocyte-like cells (arrowheads in Fig. 3B) and moderately stained neuropils (Fig. 3B) in the external plexiform layer.

3.2.2. Septum and nuclei of the diagonal band of Broca

Moderate BMP7-IR was seen in the medial septal nuclei and diagonal band of Broca (Fig. 3C). Closer observation showed that small cells were moderately stained, and moderate neuropil staining was also seen (Fig. 3D and E). In the lateral septal nucleus, small BMP7-IR positive astrocyte-like cells were evenly distributed (arrowheads in Fig. 3F). Interestingly, strong BMP7-IR was seen on ependyma of lateral ventricles (arrows in Fig. 3F). This strong ependymal staining was also observed using immunofluorescent staining (arrows in Fig. 3G).

3.2.3. Islands of Calleja

Many moderately stained cells were detected in the islands of Calleja and moderately stained neuropils were seen (Fig. 3H).

3.2.4. Cerebral cortex

Evenly distributed small cells strongly stained with BMP7 antibody and moderate neuropil staining were seen throughout the cerebral cortex (Fig. 4A). Closer observation showed that the small cells had an astrocyte-like appearance in layers I and V (arrowheads in Fig. 4B and C).

3.2.5. Hippocampus

Small BMP7-IR positive cells and weak to moderate neuropil staining were observed throughout the hippocampus (Fig. 4D). Closer observation showed strong BMP7-IR positive astrocyte-like cells in Ammon's horn (arrowheads in Fig. 4E and F); in contrast, BMP7-IR was not detected in pyramidal neurons (asterisks in Fig. 4F). Moderate neuropil staining was seen in the oriens layer (Fig. 4E and F). The dentate gyrus had strong BMP7-IR positive astrocyte-like cells (arrowheads in Fig. 4G and H), but BMP7-IR was

Table 1
Distribution and Intensity of BMP7-IR in the rat CNS.

Area	Intensity	Area	Intensity
I. Telencephalon		IV. Pons and medulla	
Olfactory bulb		Motor system	
Olfactory nerve layer	+++	Trigeminal motor nucleus	+++
Glomerular layer	++	Hypoglossal nucleus	+++
External plexiform layer	++	General somatosensory system	
Mitral cell layer	++	Trigeminal mesencephalic nucleus	+++
Granular layer	++	Trigeminal spinal nucleus	+++
Subependymal layer	++	General visceromotor system	
Cerebral cortex	++	Dorsal nucleus of the vagus	++
Hippocampal formation		General viscerosensory system	
Ammon's horn	++	The nucleus of the solitary tract	++
Dentate gyrus	+++	Special somatosensory system	
Amygdala	+	Auditory system	
Basal ganglia		Dorsal cochlear nucleus	++
Caudate putamen	++	Ventral cochlear nucleus	+++
Globus pallidus	++	Inferior colliculus	++
Ilands of Calleja	++	Vestibular system	
Corpus callosum	+++	Medial vestibular nucleus	+++
II. Diencephalon		Pontine dorsal tegmental nucleus	+++
Thalamus		Pontine nucleus	+++
Reticular nucleus	+++	Area postrema	++++
Medial habenular nucleus	++	Locus coeruleus	++++
Lateral habenular nucleus	+	Inferior olive	+++
Ventroposterior nucleus	++	V. Cerebellum	
Lateral geniculate nucleus	++	Cortex	
Other nuclei	+	Molecular layer	++++
Hypothalamus		Purkinje cell layer	++++
Paraventricular hypothalamic nucleus	+++	Granule cell layer	++
Other nuclei	+	Cerebellar nuclei	+++
Median eminence	++++	VI. Spinal cord	
III. Midbrain		Dorsal horn	+++
Red nucleus	++	Ventral horn	+++
Substantia nigra	++		
Interpeduncular nucleus	++++		
Oculomotor nucleus	+++		
Superior colliculus	++		

Relative intensities were estimated by visual comparison of immunostained slide: +, low; ++, moderate; +++, strong; ++++, very strong.

not seen in granule neurons (asterisks in Fig. 4H). Strong neuropil staining was seen in the polymorphic layer (Fig. 4G and H).

3.2.6. Basal ganglia

The caudate putamen had moderately positive small cells and moderate neuropil staining in gray matter (Fig. 5A and B), while the globus pallidus had moderately positive astrocyte-like cells (arrowheads in Fig. 5C) and weak neuropil staining in gray matter (Fig. 5C).

3.2.7. Corpus callosum

Strong BMP7-IR-positive cells were detected in the corpus callosum (arrowheads in Fig. 5D). On closer observation, these cells had an astrocyte-like appearance (arrowheads in Fig. 5E).

3.2.8. Amygdala

Weak BMP7-IR was seen in all nuclei of the amygdala (Fig. 2D).

3.3. Diencephalon

BMP7-IR positive cells and neuropils were observed in all nuclei in the thalamus (Fig. 2C and D, Fig. 5F). There were strongly positive astrocyte-like cells (arrowheads in Fig. 5G) and moderate neuropil staining in the reticular thalamic nucleus (Fig. 5G); strongly positive astrocyte-like cells and moderate neuropil staining in the ventroposterior thalamic nucleus (Fig. 5H); moderate BMP7-IR positive astrocyte-like cells and neuropils in the medial habenular nucleus (Fig. 5I and J); and moderately-stained small cells and neuropils in the lateral geniculate nucleus (Fig. 5K and L).

In the hypothalamus, we detected weak BMP7-IR in all nuclei (Fig. 2D and E). Interestingly, the magnocellular part of the paraventricular hypothalamic nucleus contained very strongly positive neurons (arrows in Fig. 6A). Closer observation showed that large neurons with varicose neurites exhibited very strong BMP7-IR (Fig. 6A and B). To determine which kinds of neurons express BMP7-IR, we performed the mirror method, in which pairs of consecutive thin sections were stained with BMP7 antibody and rabbit anti-oxytocin antibody, respectively, and found that the positive neurons are oxytocin neurons (arrowheads in Fig. 6C_1, C_2). In addition, the medial part of the median eminence showed very strong BMP7-IR (arrows in Fig. 6D). Closer observation showed many strongly stained astrocyte-like cells expressed abundant BMP7 proteins (arrowheads in Fig. 6E). This strong BMP7-IR in the median eminence was also observed using immunofluorescent staining (arrowheads in Fig. 6F).

3.4. Midbrain

Very strong BMP7-IR was detected in the interpeduncular nucleus (arrows in Fig. 7A). On closer observation, very strongly stained astrocyte-like cells (arrowheads in Fig. 7B) and very strong neuropil staining were detected (Fig. 7B). In addition, the red nucleus and substantia nigra were moderately stained (Fig. 7A). In the red nucleus, large-sized neurons exhibited strong BMP7-IR (arrowheads in Fig. 7C), while weak BMP7-IR was detected in neuropils (Fig. 7C). Strongly-stained neurons (arrowheads in Fig. 7D) and weak neuropil staining (Fig. 7D) were observed in the pars compacta of the substantia nigra. The superior colliculus showed
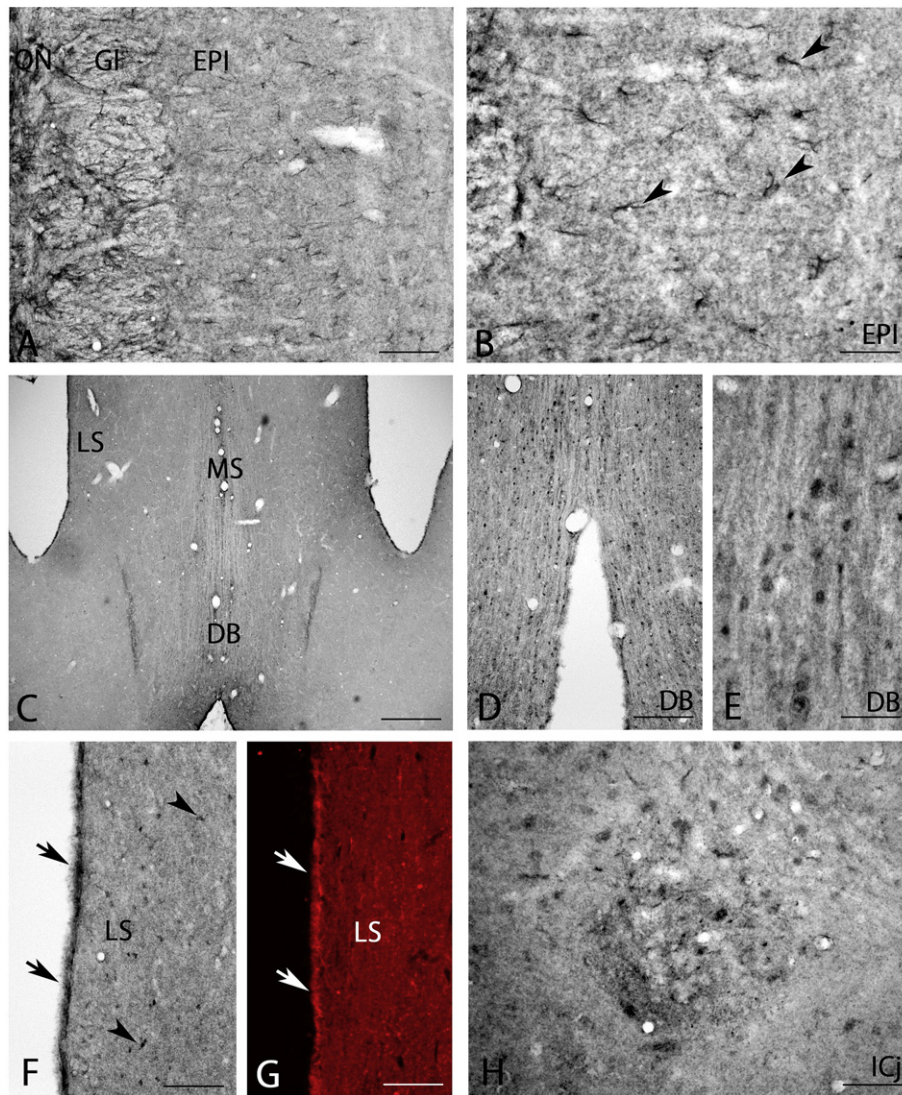
Fig. 3. BMP7 expression in the olfactory bulb (A, B), medial septal nucleus (C), diagonal band (D, E), lateral septal nucleus (F, G), and islands of Calleja (H). Astrocyte-like cells were strongly stained in the external plexiform layer (arrowheads in B) and the lateral septal nucleus (arrowheads in F), and the ependyma of the lateral ventricle (arrows in F and G) was very strongly stained. DB, diagonal band; EPI, external plexiform layer; Gl, glomerular layer; ICj, islands of Calleja; LS, lateral septal nucleus; MS, medial septal nucleus; ON, olfactory nerve layer. Scale bar = 160 μm for C; 80 μm for A, D, F; 40 μm for B, E, G, H.

moderate BMP7-IR (Fig. 7E). Interestingly, the superficial part of the superior colliculus showed strong BMP7-IR (Fig. 7E). In addition, strong BMP7-IR was observed in the pia mater of the superior colliculus (arrows in Fig. 7E). This strong BMP7-IR in the pia mater was also observed using immunofluorescent staining (arrows in Fig. 7F). Furthermore, the oculomotor nucleus exhibited abundant BMP7-IR in neuronal cell bodies and neuropils (Fig. 7G).

3.5. Pons and medulla

3.5.1. Motor system

Nuclei in the general somatomotor and brachiomotor system, such as the motor trigeminal nucleus (Fig. 7H) and hypoglossal nucleus (Fig. 7J), showed abundant BMP7-IR in neuronal cell bodies and neuropils. Interestingly, the facial nerve showed strong BMP7-IR in axon fibers (arrows in Fig. 7I).

3.5.2. General somatosensory system

Large primary afferent neurons were strongly stained in the trigeminal mesencephalic nucleus (arrowheads in Fig. 7K), with

scattered strongly stained astrocyte-like cells (Fig. 7K). The trigeminal spinal nucleus had strongly stained small cells and neuropils (Fig. 7L, M), and strongly stained axons were also seen in the medial lemniscus (arrows in Fig. 7N).

3.5.3. General visceromotor system

Moderate BMP7-IR positive neurons and weak neuropil staining were observed in the dorsal nucleus of the vagus (Fig. 8A).

3.5.4. General viscerosensory system

Moderate BMP7-IR small cells and moderate neuropil staining were seen in the nucleus of the solitary tract (Fig. 8A and B).

3.5.5. Special somatosensory system

Auditory system: Ventral cochlear nuclei had strong BMP7-IR staining (Fig. 8C) and dorsal cochlear nuclei had moderate BMP7-IR (Fig. 8D). Moderate BMP7-IR was detected in the inferior colliculus and strong BMP7-IR staining was seen in the superior olive (Fig. 8E).

Vestibular system: Strongly stained axons were seen in the vestibulocochlear nerve (arrows in Fig. 8F) and there was strong
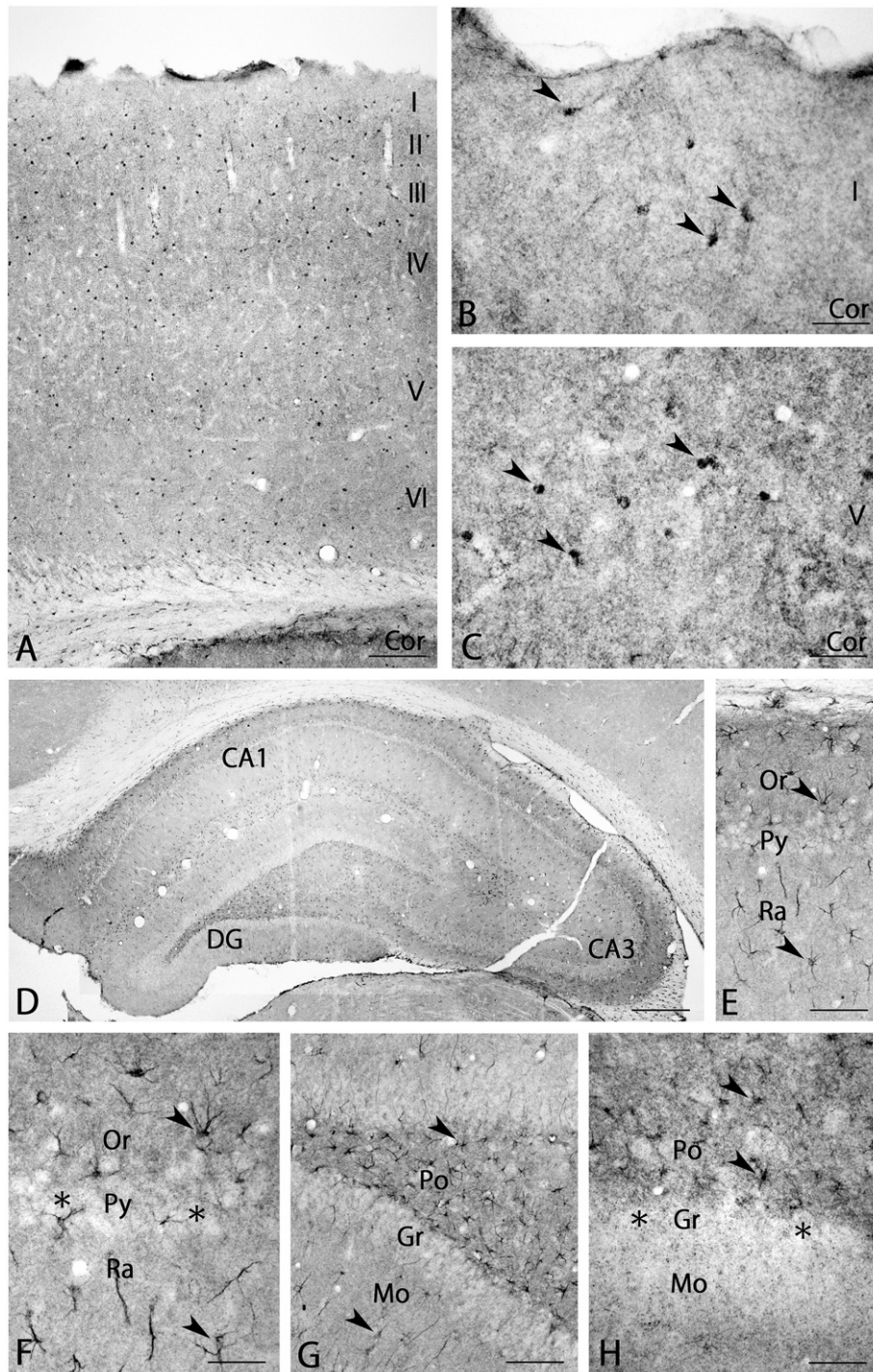
Fig. 4. BMP7 expression in the cerebral cortex (A–C) and hippocampus (D–H). Astrocyte-like cells in the cerebral cortex (arrowheads in B and C) and in the hippocampus (arrowheads in E-H) were strongly stained, and pyramidal neurons (asterisks in F) and granule neurons (asterisks in H) in the hippocampus were not stained. I-VI, layers I-VI; CA1, 3, field CA1, 3 of Ammon's horn; DG, dentate gyrus; Gr, granular layer; Mo, stratum molecular; Or, stratum oriens; Po, polymorphic layer; Py, stratum pyramidale; Ra, stratum radiatum. Scale bar = 400 μm for D; 160 μm for A; 80 μm for E, G; 40 μm for B, C, F, H.

BMP7-IR in the medial vestibular nucleus (Fig. 8G) and in the ependyma of the fourth ventricle (arrowheads in Fig. 8G). This strong ependymal BMP7-IR was also seen using immunofluorescent staining (arrows in Fig. 8H).

3.5.6. Other lower brain stem areas

Strong BMP7-IR was observed in the pontine dorsal tegmental nucleus (Fig. 9A) and pontine nucleus (Fig. 9B). Closer observation also showed strongly-stained small cells and neuropils in the pontine nucleus (Fig. 9B and C). In addition, very strong BMP7-IR was observed in the area postrema (Fig. 9D) and there were very strongly stained neurons and neuropils in the locus coeruleus (Fig. 9E), and strongly stained neurons and moderate neuropil staining in the inferior olive (Fig. 9F and G). Interestingly, there were also many BMP7-IR axons in the inferior cerebellar peduncle, which originates from the inferior olive (arrows in Fig. 9H).
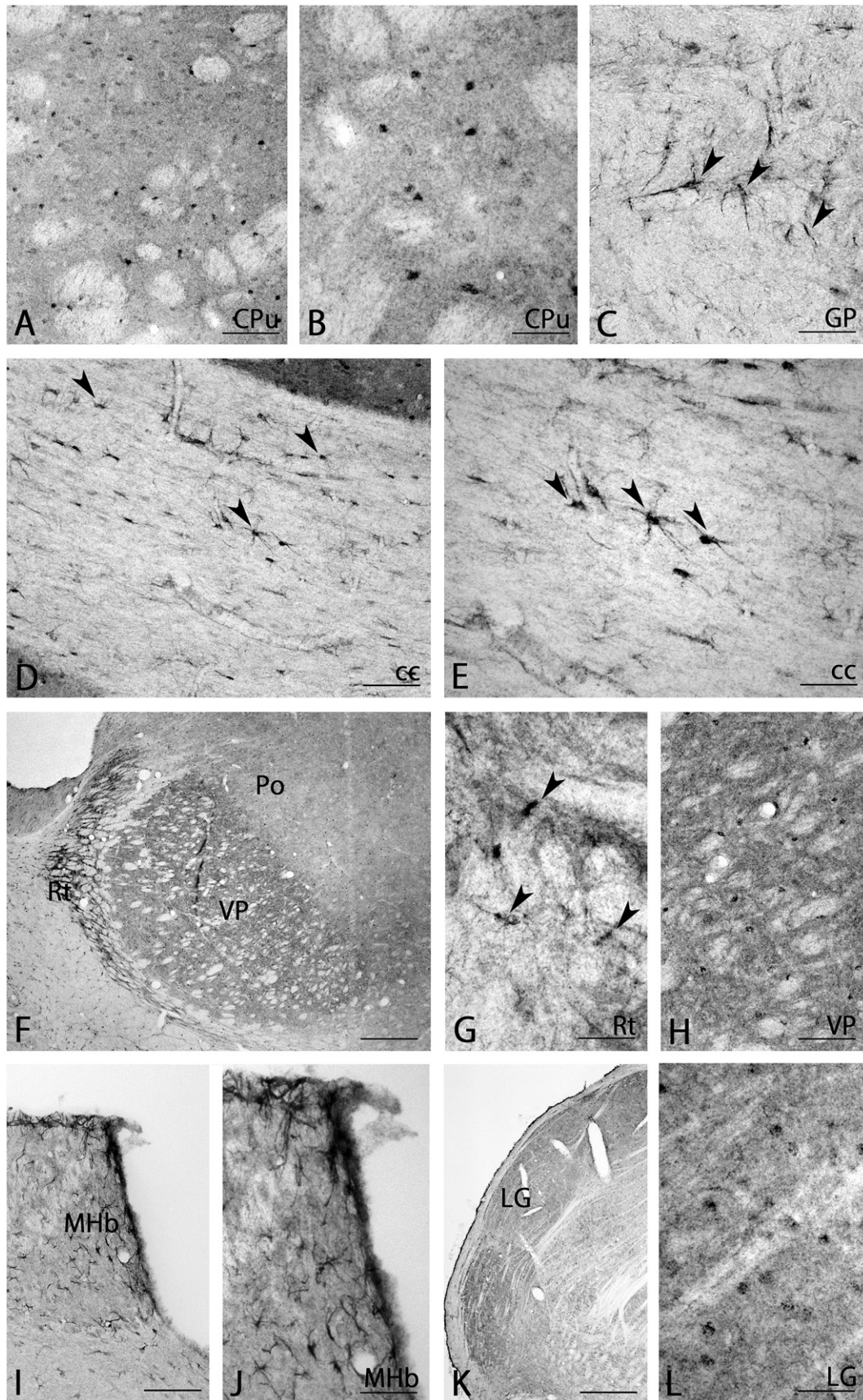
Fig. 5. BMP7 expression in the basal ganglia (A–C), corpus callosum (D, E), and thalamus (F–L). Moderately positive astrocyte-like cells were seen in the globus pallidus (arrowheads in C), and astrocyte-like cells in the corpus callosum (arrowheads in D and E) and reticular thalamus (arrowheads in G) were strongly stained. cc, corpus callosum; CPu, caudate putamen; GP, globus pallidus; LG, lateral geniculate nucleus; MHb, medial habenular nucleus; Po, posterior thalamic nucleus; Rt, reticular thalamic nucleus; VP, ventroposterior thalamic nucleus. Scale bar = 400 μm for F, K; 80 μm for A, D, H, I; 40 μm for B, C, E, G, J, L.
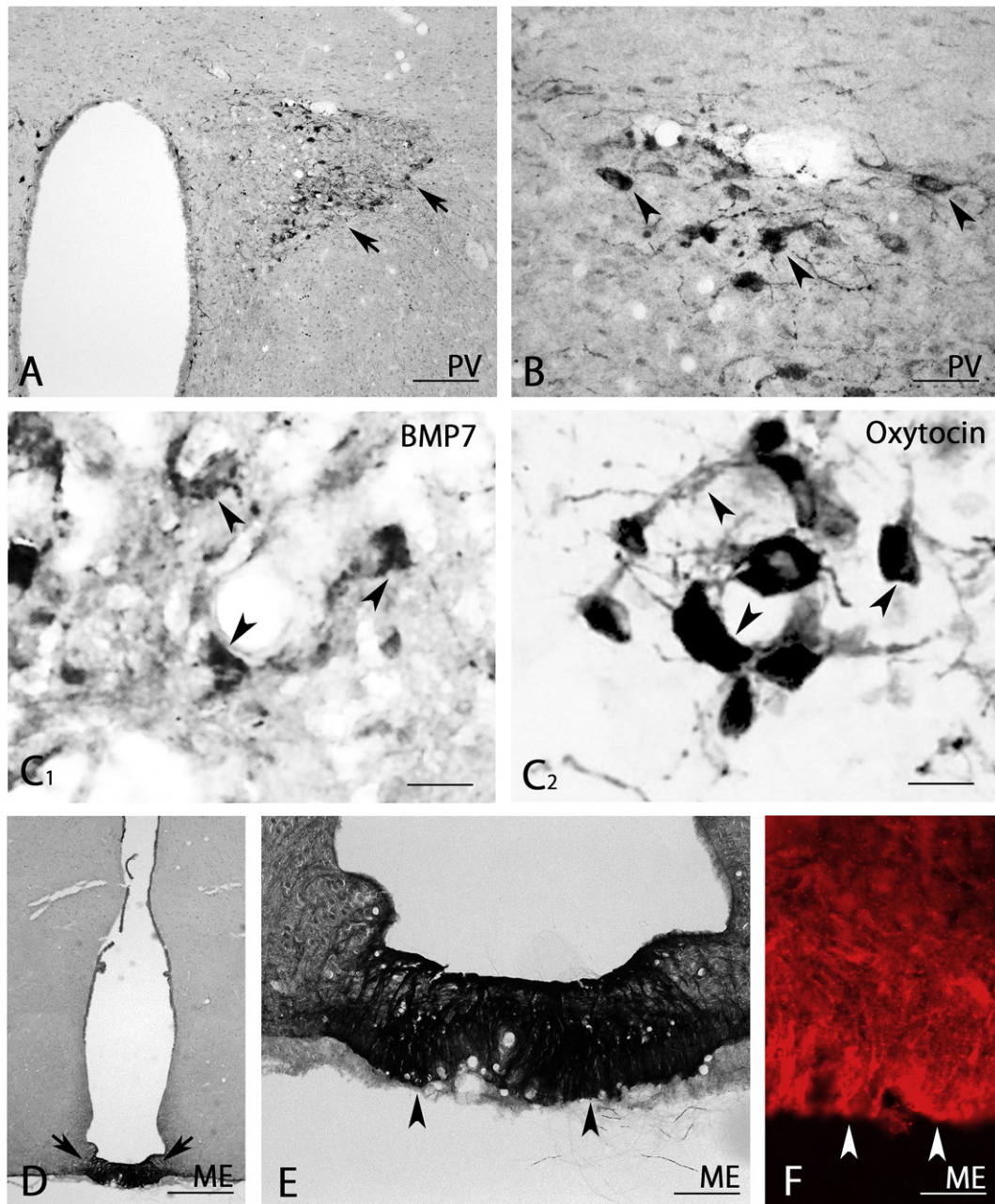
Fig. 6. BMP7 expression in the hypothalamus (A–F). Large neurons in the magnocellular part of the paraventricular hypothalamic nucleus were very strongly stained (arrowheads in B), and the medial part of the median eminence was also very strongly stained (arrows in D). The mirror method showed that the positive neurons were oxytocin neurons (arrowheads in C_1 and C_2). PV, paraventricular hypothalamic nucleus; ME, medial eminence. Scale bar = 400 μm for D; 160 μm for A; 80 μm for E; 40 μm for B; 20 μm for C_1, C_2, F.

3.6. Cerebellum

There was very strong BMP7-IR in the Purkinje cell layer and the molecular cell layer in the cerebellum. Cell bodies of Purkinje neurons (arrows in Fig. 10A) and Bergmann glias around these cell bodies exhibited very strong BMP7-IR (arrowheads in Fig. 10A). Moderate BMP7-IR was seen in the granular cell layer (Fig. 10A). Cerebellar nuclei had strong BMP7-IR positive neurons (arrowheads in Fig. 10B) and moderate neuropil staining (Fig. 10B).

3.7. Spinal cord

There was strong BMP7-IR in the gray matter of the spinal cord, while BMP7 expression in the white matter was relatively weak (Fig. 10C). Strong positive cells and neuropils were detected in the dorsal horn (Fig. 10D) and the ventral horn (Fig. 10E). Closer observation showed that large motor neurons expressed BMP7-IR (arrowheads in Fig. 10F). Astrocyte-like cells (arrowheads in Fig. 10G) and axons (arrows in Fig. 10G) were stained in the white matter.

3.8. Other areas

In the subventricular zone (SVZ), moderately stained astrocyte-like cells were detected (arrowheads in Fig. 10H). Ependymal cells were moderately stained (arrows in Fig. 10H) and the choroidal plexus also expressed abundant BMP7 (arrowheads in Fig. 10I).
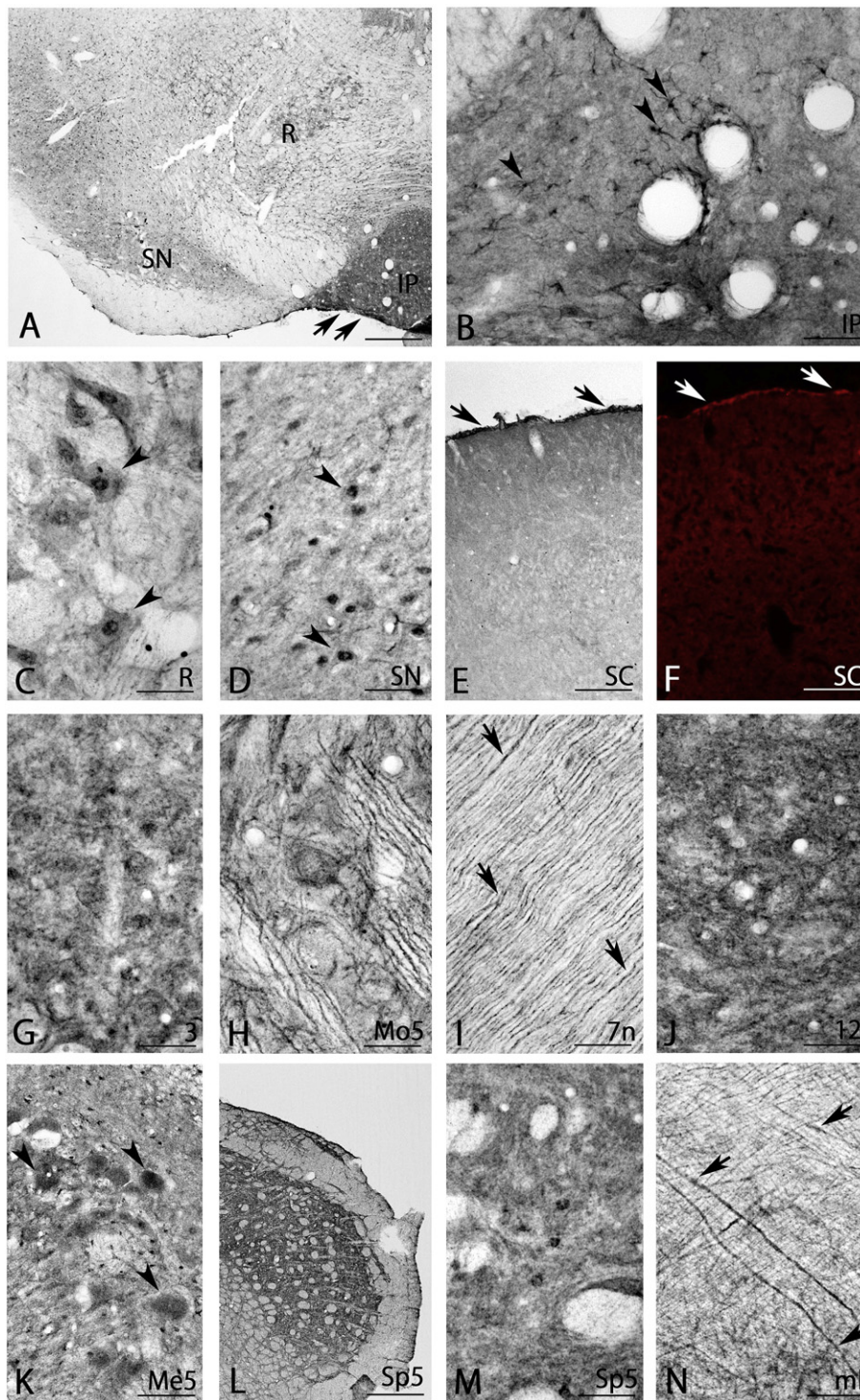
Fig. 7. BMP7 expression in the midbrain (A–D), superior colliculus (E, F), motor system (G–J) and general somatosensory system (K–N). Astrocyte like cells in the interpeduncular nucleus were very strongly stained (arrowheads in B), and neurons in the red nucleus (arrowheads in C), pars compacta of the substantia nigra (arrowheads in D), pia mater of the superior colliculus (arrows in E and F); the axons in the facial nerve (arrows in I); neurons in the trigeminal mesencephalic nucleus (arrowheads in K); and axons in the medial lemniscus (arrows in N) were strongly stained. 3, oculomotor nucleus; 7n, facial nerve; 12, hypoglossal nucleus; IP, interpeduncular nucleus; Me5, trigeminal mesencephalic nucleus; ml, medial lemniscus; Mo5, motor trigeminal nucleus; R, red nucleus; SC, superior colliculus; SN, substantia nigra; Sp5, trigeminal spinal nucleus. Scale bar = 400 μm for A; 160 μm for E, L; 80 μm for F; 40 μm for B-D, G-K, M, N.

3.9. Double fluorescence immunohistochemistry

Many astrocyte-like cells were detected throughout the CNS. To show that these cells are actually astrocytes, double fluorescence IHC with anti-GFAP antibody was performed in the cerebral cortex, hippocampus, corpus callosum and cerebellum. As shown in Fig. 11A–D, co-expression of BMP7 and GFAP was observed in these regions, indicating that astrocytes express BMP7. To further examine BMP7 expression in astrocytes in the cortex, hippocampus, and corpus callosum, we combined nuclear staining using
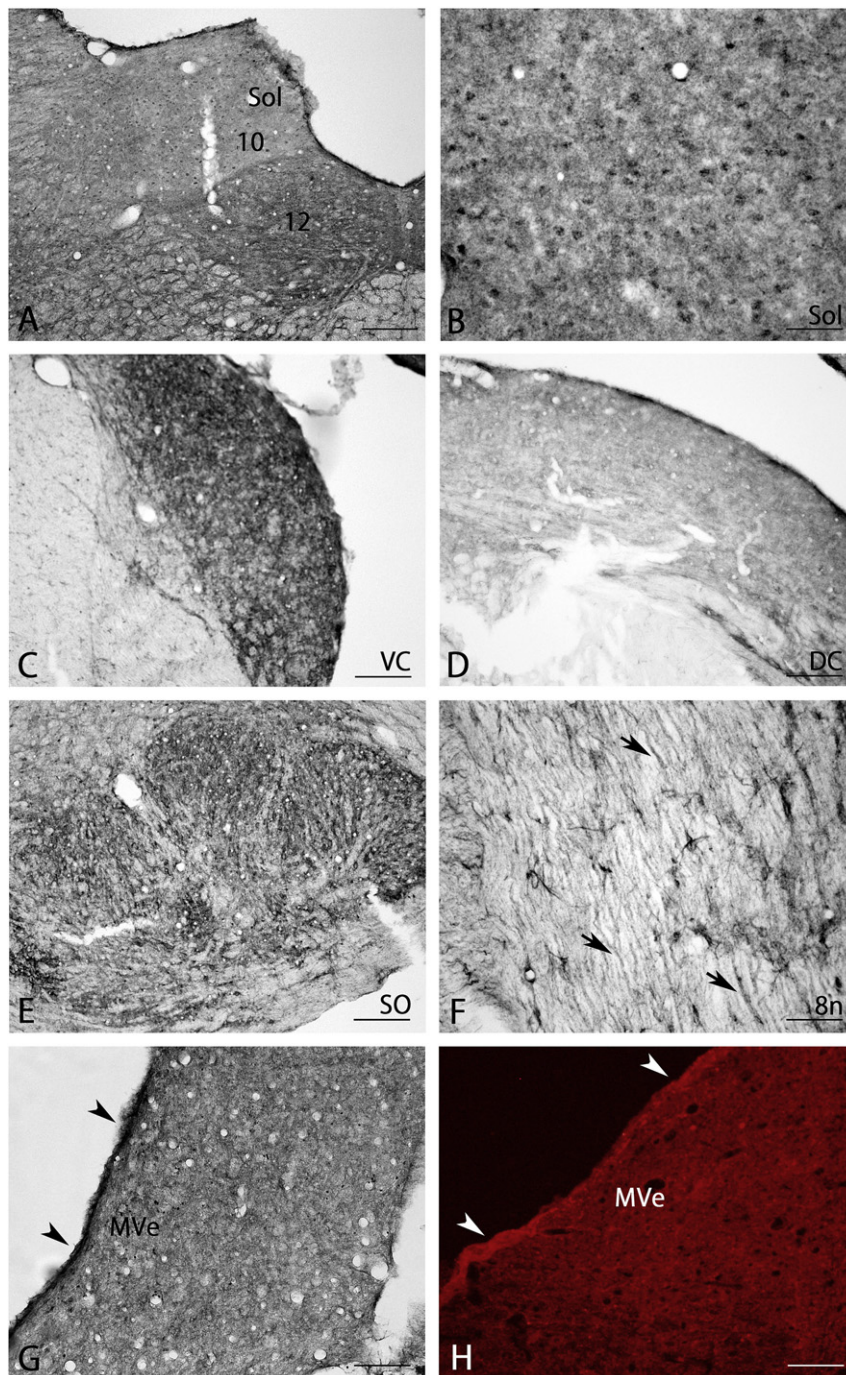
Fig. 8. BMP7 expression in the general viscerosensory system (A, B) and special somatosensory system (C–H). Axons in the vestibulocochlear nerve (arrows in F) and ependyma of the fourth ventricle (arrowheads in G and H) were strongly stained. 8n, vestibulocochlear nerve; 10, vagus nucleus; 12, hypoglossal nucleus; DC, dorsal cochlear nucleus; MVe, medial vestibular nucleus; SO, superior olive; Sol, nucleus of the solitary tract; VC, ventral cochlear nucleus. Scale bar = 160 μm for A, C, D; 80 μm for E, G; 40 μm for B, F, H.

4′, 6-diamidino-2-phenylindole (DAPI) with double fluorescence IHC with anti-GFAP antibody. In these regions, BMP7-IR was only detected in cells positive for GFAP (Fig. 12A–C), further indicating that astrocytes express BMP7. Double fluorescence IHC with anti-Iba1 antibody (microglial marker) was also performed, but Iba1-positive microglial cells did not show any BMP7-IR (Fig. 12D).

4. Discussion

In this study, we showed that BMP7 is widely expressed in the adult CNS. Interestingly, abundant BMP7 expression in astrocytes

was found throughout the CNS, in addition to staining for BMP7 in certain neuronal cell bodies, axons, ependymal cells and meninges.

4.1. BMP7 expression in astrocytes

Strong BMP7 expression in astrocytes was observed throughout the CNS. In the cortex and hippocampus, many strongly stained astrocytes were present, but BMP7 expression in neurons was not detected. These results suggest that astrocytes are the main suppliers of BMP7 in the CNS. Interestingly, BMP7 is known to regulate astrocytes. For example, Yanagisawa et al. (2001) found that BMP7
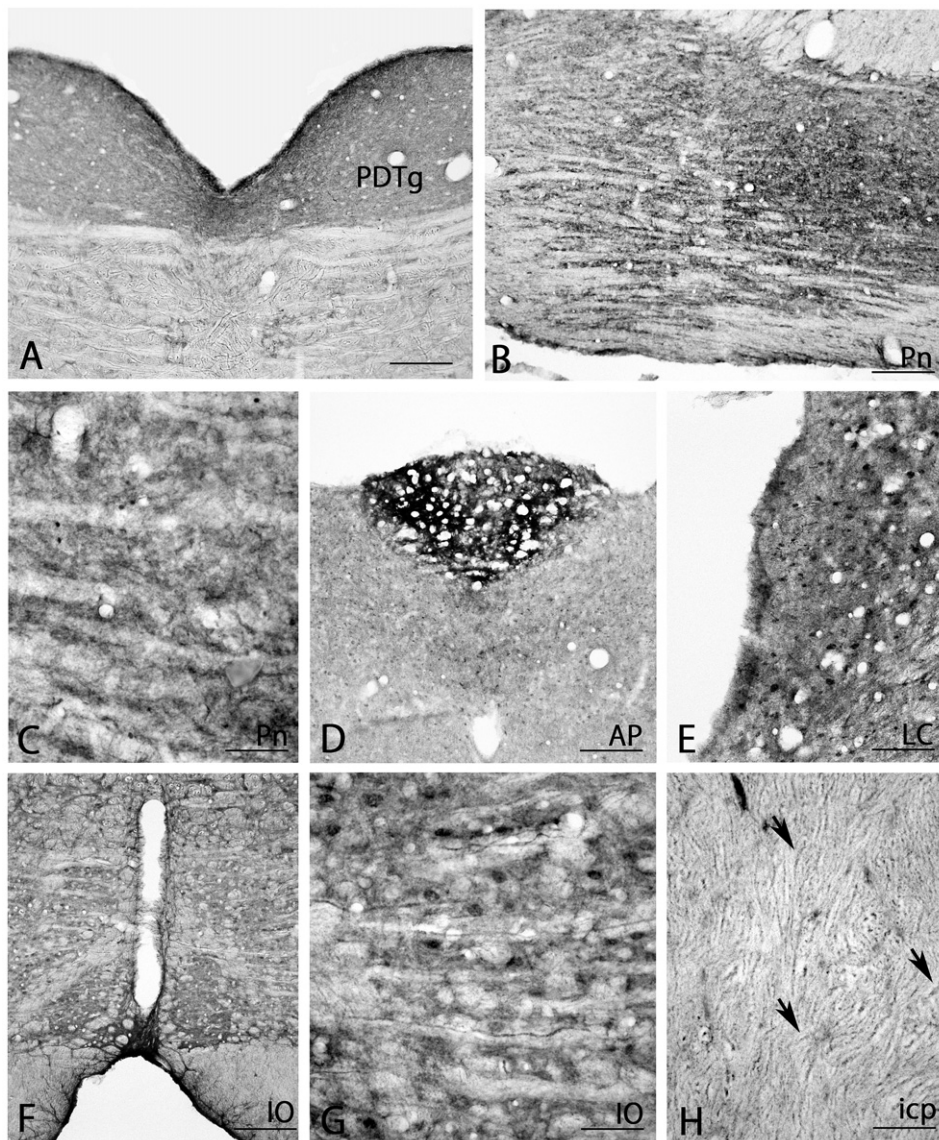
Fig. 9. BMP7 expression in other lower brain stem areas (A–H). Axons in the inferior cerebellar peduncle (arrows in H) were moderately stained. AP, area postrema; icp, inferior cerebellar peduncle; IO, inferior olive; LC, locus coeruleus; PDTg, pontine dorsal tegmental nucleus; Pn, pontine nucleus. Scale bar = 160 μm for A, B, D, F; 80 μm for E; 40 μm for C, G, H.

inhibits neurogenesis and concomitantly induces astrocytogenesis of mouse fetal neuroepithelial cells. In addition, in the developing cerebral cortex, BMP7 induces premature radial glia differentiation and impairs neuronal migration (Ortega and Alcantara, 2010). These reports show that BMP7 is highly involved in differentiation of astrocytes.

BMP7 is also involved in gliosis. For example, BMP7 increases the levels of proteins associated with reactive gliosis in retinal astrocytes and Müller glial cells, including GFAP, glutamine synthetase, a subset of chondroitin sulfate proteoglycans (CSPGs), matrix metalloproteinases, and other molecules (Dharmarajan et al., 2014). Local increases in BMP7 at the site of a demyelinating lesion cause upregulation of gliosis, glial scar formation, and increased levels of CSPGs such as neurocan and aggrecan, which may inhibit remyelination (Fuller et al., 2007). Taken together, these results suggest that BMP7 released from astrocytes may then regulate the astrocytes themselves under normal and pathological conditions.

4.2. BMP7 expression in neurons

BMP7 was not detected in many kinds of neurons, including those in the cerebral cortex and hippocampus, but was found abundantly in oxytocin, noradrenergic and dopamine neurons. Liu and Placzek (2014) found that BMP7 acts as a cue to direct hypothalamic neurosecretory axons into the medial ventral midline of the hypothalamus through repulsion. Interestingly, we found intense BMP7 expression in oxytocin neurons in the magnocellular part of the paraventricular hypothalamic nucleus and astrocytes in the medial part of the median eminence (Fig. 6). Since axons of oxytocin and vasopressin neurons pass through this medial region, BMP7 in oxytocin neurons and the medial part of the medial eminence may be necessary to keep the trajectories of axons of these neurons to the posterior lobe of the pituitary.

BMP7 is also a critical mediator of catecholaminergic neuron differentiation. Deletion of BMP7 and BMP5 genes results in an absence of noradrenergic neurons in the locus coeruleus
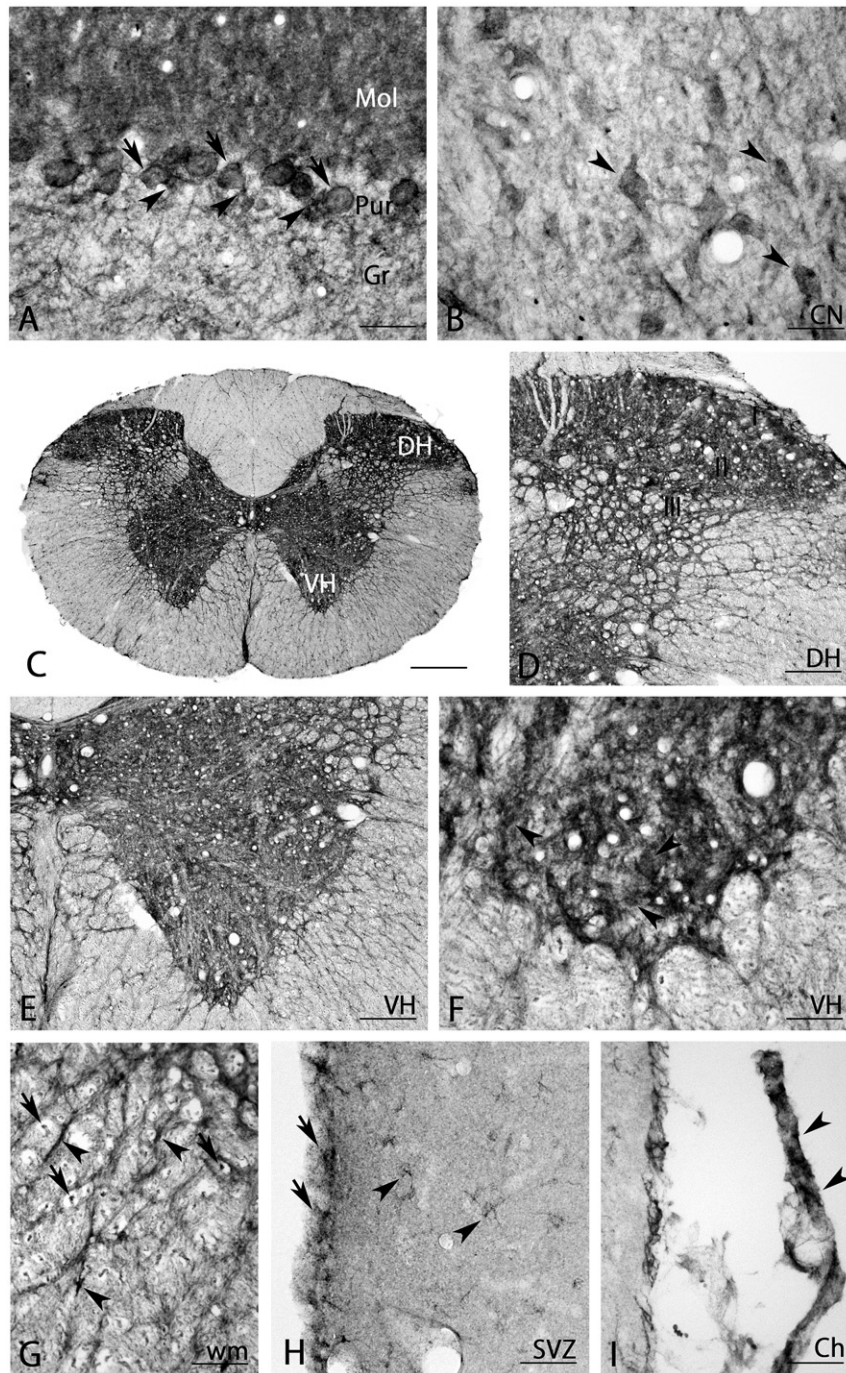
Fig. 10. BMP7 expression in the cerebellum (A, B), spinal cord (C–G), subventricular zone (H) and choroidal plexus (I). Purkinje cells (arrows in A) and Bergmann glias around the cell bodies of Purkinje cells (arrowheads in A) were very strongly stained, and neuronal cell bodies in cerebellar nuclei (arrowheads in B), neurons in the ventral horn (arrowheads in F), astrocyte-like cells in the white matter (arrowheads in G), and axons in the white matter (arrows in G) were strongly stained. I-III, layers I-III of the spinal cord; Ch, choroidal plexus; CN, cerebellar nuclei; DH, dorsal horn; Gr, granular layer; Mol, molecular layer; Pur, Purkinje cell layer; SVZ, subventricular zone; VH, ventral horn; wm, white matter. Scale bar = 400 μm for C; 80 μm for D, E; 40 μm for A, B, F, G-I.

(Tilleman et al., 2010). In addition, BMP7 induces dendritic growth of noradrenergic neurons (Lein et al., 1995, 2002) and protects these neurons against 6-hydroxydopamine-induced neurotoxicity (Harvey et al., 2004). Jordan et al. (1997) showed that application of BMP7 to rat mesencephalic cell cultures increases both the number of tyrosine hydroxylase-expressing cells and dopamine uptake. These reports show that BMP7 has important roles in noradrenergic and dopamine neurons, and may be needed to maintain the identities of these catecholaminergic neurons.

4.3. BMP7 expression in axons

BMP7 was expressed in many kinds of axons, such as these in the facial nerve (Fig. 7I) and vestibulocochlear nerve (Fig. 8F). Retrograde BMP signal transduction through axons has been shown to modulate neuronal terminal differentiation and synaptic efficacy (da Silva and Wang, 2011). In Drosophila, McCabe et al. (2003) found that a muscle-derived BMP homolog, Glass bottom boat (Gbb), participates in coordinating neuromuscular
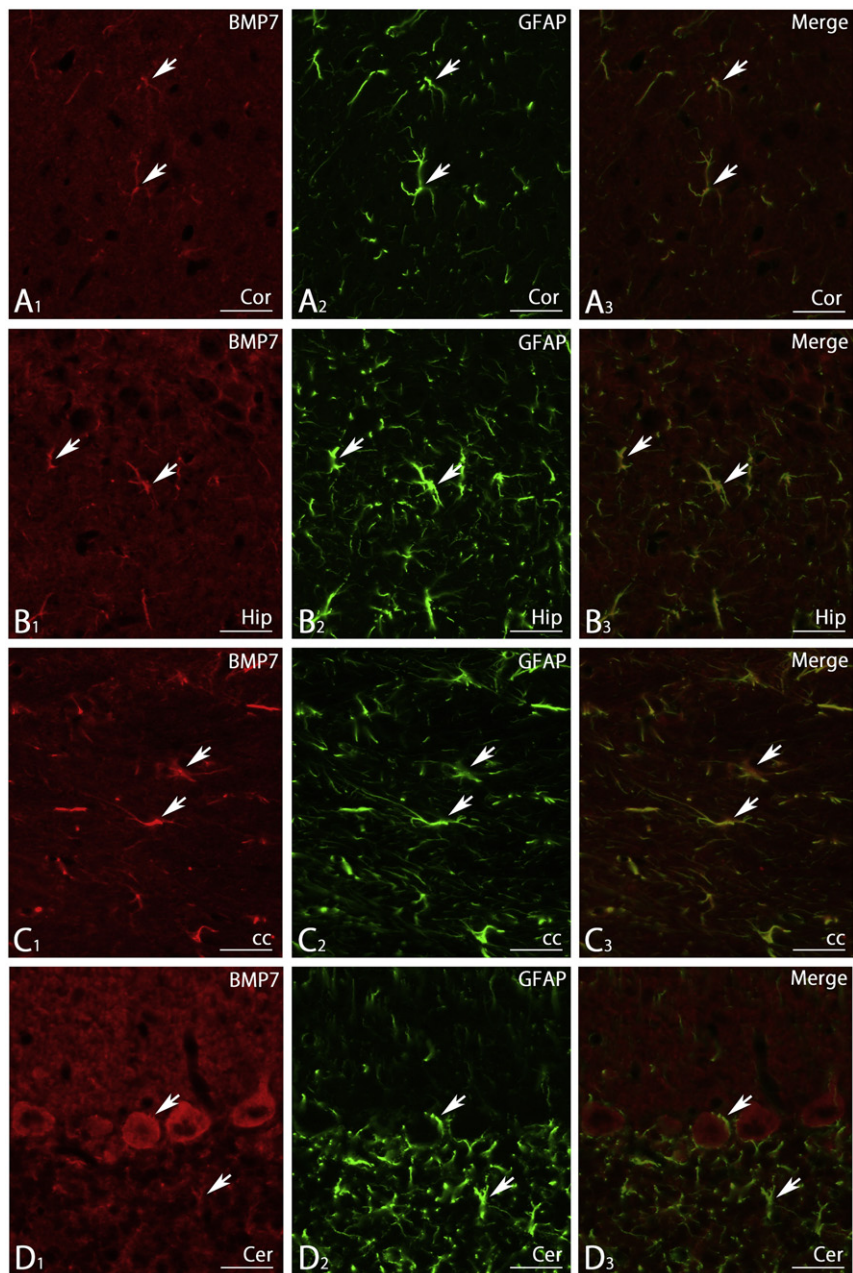
Fig. 11. Double staining showing that BMP7-IR positive cells in the cerebral cortex (A_1), hippocampus (B_1), corpus callosum (C_1) and cerebellum (D_1) are also positive for GFAP (A_2-D_2) in a merged photomicrograph (A_3-D_3). cc, corpus callosum; Cer, cerebellum; Cor, cerebral cortex; Hip, hippocampus. Scale bar = 20 μm.

synapse development and growth. In mice, target-derived BMP signaling controls development of trigeminal ganglia and sensory innervation of the skin (Guha et al., 2004), and regulates spatial patterns of gene expression in trigeminal ganglia (Hodge et al., 2007). These data suggest that BMP7 released from postsynaptic neurons or surrounding astrocytes may be taken up by presynapses and may function in retrograde signaling. In support of this speculative role for BMP7, Tsai et al. (2010) found that BMP7 overexpression mediated through adenoviral gene transfer to sciatic nerves protects against axonal and myelin degeneration and improves functional recovery after sciatic nerve injury in rats.
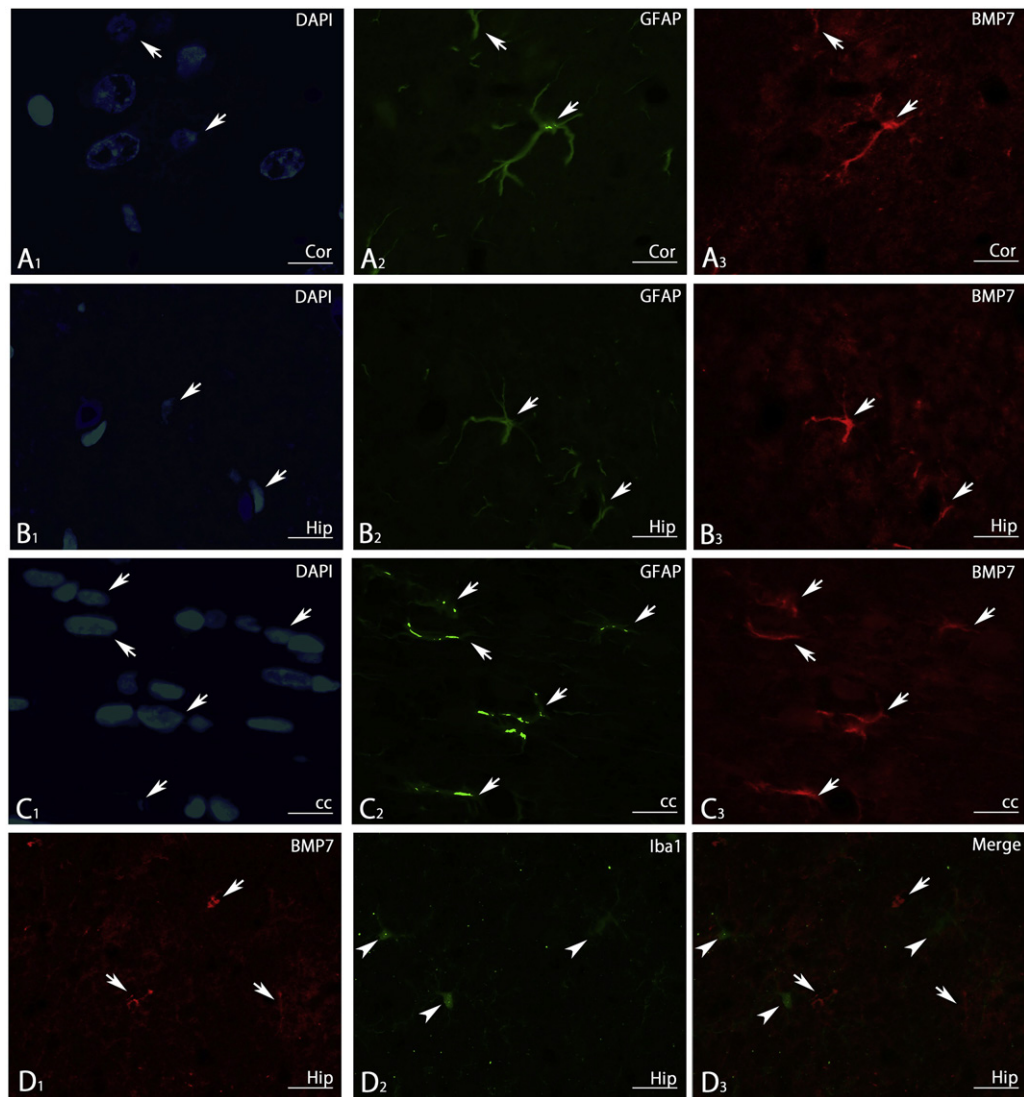
Fig. 12. Immunofluorescence staining showing that BMP7-IR positive cells in the cerebral cortex (A), hippocampus (B) and corpus callosum (C) are astrocytes based on nuclear staining using DAPI, and that BMP7-IR positive cells in the hippocampus (D_1) are not positive for Iba1 (D_2) in a merged photomicrograph (D_3). cc, corpus callosum; Cor, cerebral cortex; DAPI, 4′, 6-diamidino-2-phenylindole; Hip, hippocampus. Scale bar = 20 μm for D; 8 μm for A–C.

References

Bragdon, B., Moseychuk, O., Saldanha, S., King, D., Julian, J., Nohe, A., 2011. Bone morphogenetic proteins: a critical review. Cell Signal. 23, 609–620.

Cho, K.W., Blitz, I.L., 1998. BMPs, Smads and metalloproteases: extracellular and intracellular modes of negative regulation. Curr. Opin. Genet. Dev. 8, 443–449.

Courter, L.A., Shaffo, F.C., Ghogha, A., Parrish, D.J., Lorentz, C.U., Habecker, B.A., Lein, P.J., 2016. BMP7-induced dendritic growth in sympathetic neurons requires p75(NTR) signaling. Dev. Neurobiol. 76, 1003–1013.

da Silva, S., Wang, F., 2011. Retrograde neural circuit specification by target-derived neurotrophins and growth factors. Curr. Opin. Neurobiol. 21, 61–67.

Dharmarajan, S., Gurel, Z., Wang, S., Sorenson, C.M., Sheibani, N., Belecky-Adams, T.L., 2014. Bone morphogenetic protein 7 regulates reactive gliosis in retinal astrocytes and Müller glia. Mol. Vis. 20, 1085–1108.

Dudley, A.T., Lyons, K.M., Robertson, E.J., 1995. A requirement for bone morphogenetic protein-7 during development of the mammalian kidney and eye. Genes Dev. 9, 2795–2807.

Fuller, M.L., DeChant, A.K., Rothstein, B., Caprariello, A., Wang, R., Hall, A.K., Miller, R.H., 2007. Bone morphogenetic proteins promote gliosis in demyelinating spinal cord lesions. Ann. Neurol. 62, 288–300.

Guha, U., Gomes, W.A., Samanta, J., Gupta, M., Rice, F.L., Kessler, J.A., 2004. Target-derived BMP signaling limits sensory neuron number and the extent of peripheral innervation in vivo. Development 131, 1175–1186.

Harvey, B.K., Mark, A., Chou, J., Chen, G.J., Hoffer, B.J., Wang, Y., 2004. Neurotrophic effects of bone morphogenetic protein-7 in a rat model of Parkinson's disease. Brain Res. 1022, 88–95.

Hodge, L.K., Klassen, M.P., Han, B.X., Yiu, G., Hurrell, J., Howell, A., Rousseau, G., Lemaigre, F., Tessier-Lavigne, M., Wang, F., 2007. Retrograde BMP signaling regulates trigeminal sensory neuron identities and the formation of precise face maps. Neuron 55, 572–586.

Jordan, J., Böttner, M., Schluesener, H.J., Unsicker, K., Krieglstein, K., 1997. Bone morphogenetic proteins: neurotrophic roles for midbrain dopaminergic neurons and implications of astroglial cells. Eur. J. Neurosci. 9, 1699–1710.

Lein, P., Johnson, M., Guo, X., Rueger, D., Higgins, D., 1995. Osteogenic protein-1 induces dendritic growth in rat sympathetic neurons. Neuron 15, 597–605.

Lein, P.J., Beck, H.N., Chandrasekaran, V., Gallagher, P.J., Chen, H.L., Lin, Y., Guo, X., Kaplan, P.L., Tiedge, H., Higgins, D., 2002. Glia induce dendritic growth in cultured sympathetic neurons by modulating the balance between bone morphogenetic proteins (BMPs) and BMP antagonists. J. Neurosci. 22, 10377–10387.

Liu, F., Placzek, M., 2014. Axon guidance effects of classical morphogens Shh and BMP7 in the hypothalamo-pituitary system. Neurosci. Lett. 562, 108–113.

Massague, J., 2003. Integration of Smad and MAPK pathways: a link and a linker revisited. Genes Dev. 17, 2993–2997.

McCabe, B.D., Marques, G., Haghighi, A.P., Fetter, R.D., Crotty, M.L., Haerry, T.E., Goodman, C.S., O'Connor, M.B., 2003. The BMP homolog Gbb provides a retrograde signal that regulates synaptic growth at the Drosophila neuromuscular junction. Neuron 39, 241–254.

Moustakas, A., Heldin, C.H., 2009. The regulation of TGFbeta signal transduction. Development 136, 3699–3714.

Ortega, J.A., Alcantara, S., 2010. BDNF/MAPK/ERK-induced BMP7 expression in the developing cerebral cortex induces premature radial glia differentiation and impairs neuronal migration. Cereb. Cortex 20, 2132–2144.

Tilleman, H., Hakim, V., Novikov, O., Liser, K., Nashelsky, L., Di Salvio, M., Krauthammer, M., Scheffner, O., Maor, I., Mayseless, O., Meir, I., Kayam, G., Sela-Donenfeld, D., Simeone, A., Brodski, C., 2010. Bmp5/7 in concert with the mid-hindbrain organizer control development of noradrenergic locus coeruleus neurons. Mol. Cell Neurosci. 45, 1–11.

Tsai, M.J., Pan, H.A., Liou, D.Y., Weng, C.F., Hoffer, B.J., Cheng, H., 2010. Adenoviral gene transfer of bone morphogenetic protein-7 enhances functional recovery after sciatic nerve injury in rats. Gene Ther. 17, 1214–1224.

Ueki, T., Tanaka, M., Yamashita, K., Mikawa, S., Qiu, Z.F., Maragakis, N.J., Hevner, R.F., Miura, N., Sugimura, H., Sato, K., 2003. A novel secretory factor, neurogenesin-1, provides neurogenic environmental cues for neural stem cells in the adult hippocampus. J. Neurosci. 23, 11732–11740.

Yanagisawa, M., Takizawa, T., Ochiai, W., Uemura, A., Nakashima, K., Taga, T., 2001. Fate alteration of neuroepithelial cells from neurogenesis to astrocytogenesis by bone morphogenetic proteins. Neurosci. Res. 41, 391–396.